

Cu nuclear spin-spin coupling in the dimer singlet state in $\text{SrCu}_2(\text{BO}_3)_2$

This article has been downloaded from IOPscience. Please scroll down to see the full text article.

2002 J. Phys.: Condens. Matter 14 L319

(<http://iopscience.iop.org/0953-8984/14/17/101>)

View [the table of contents for this issue](#), or go to the [journal homepage](#) for more

Download details:

IP Address: 171.66.16.104

The article was downloaded on 18/05/2010 at 06:32

Please note that [terms and conditions apply](#).

LETTER TO THE EDITOR

Cu nuclear spin–spin coupling in the dimer singlet state in $\text{SrCu}_2(\text{BO}_3)_2$

K Kodama, J Yamazaki, M Takigawa¹, H Kageyama, K Onizuka and Y Ueda

Institute for Solid State Physics, University of Tokyo, 5-1-5 Kashiwanoha, Kashiwa-shi, Chiba 277-8581, Japan

E-mail: masashi@issp.u-tokyo.ac.jp (M Takigawa)

Received 25 March 2002

Published 18 April 2002

Online at stacks.iop.org/JPhysCM/14/L319

Abstract

We report results of nuclear magnetic resonance experiments in $\text{SrCu}_2(\text{BO}_3)_2$, a quasi-two-dimensional spin system with a singlet ground state. When magnetic field is applied along the c -axis, each of the quadrupole-split Cu resonance lines splits further into four lines. The spin-echo intensity for some of the split lines oscillates against the separation time between $\pi/2$ and π rf pulses. These phenomena are due to strong nuclear spin–spin coupling mediated by the electronic spin system, which exists only within a pair of nuclei. Thus the results provide direct evidence for the dimer singlet ground state in this material.

The discovery of an excitation gap and quantized magnetization plateaus in the quasi-two-dimensional spin system $\text{SrCu}_2(\text{BO}_3)_2$ by Kageyama *et al* [1] has stimulated a vast amount of experimental and theoretical work. As shown in figure 1, the Cu^{2+} spins ($s = 1/2$) in this compound form a planar network of dimers, which is identical to the Shastry–Sutherland (SS) model [2] when only the nearest-neighbour intra-dimer exchange (J) and the second-nearest inter-dimer exchange (J') interactions are retained.

Extensive studies on the SS model have revealed interesting novel aspects [3–11]. First, the simple direct product of the dimer singlet is an exact eigenstate for any value of J'/J and is the ground state when J'/J is smaller than a certain critical value [2, 4]. In the opposite limits, $J'/J \gg 1$, the model reduces to the nearest-neighbour Heisenberg model on a square lattice with the obvious Néel order. It was proposed that the two phases are separated by a first-order transition at $T = 0$ near $J'/J = 0.7$ [4]. For $\text{SrCu}_2(\text{BO}_3)_2$, the exponential decrease of susceptibility and Cu nuclear spin–lattice relaxation rate at low temperatures [1] indicate that the ground state is a singlet with a finite energy gap for excited states. The magnitude of

¹ Author to whom any correspondence should be addressed.

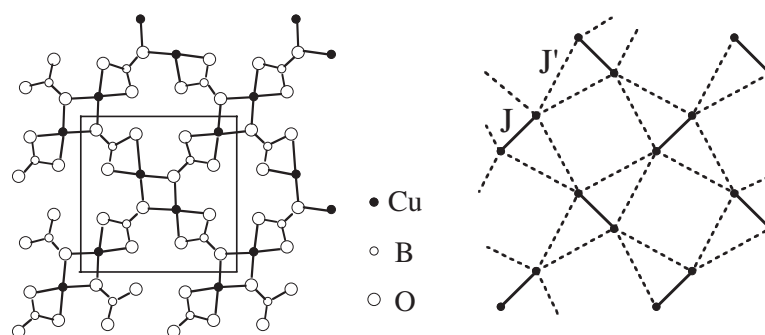


Figure 1. Structure of the magnetic layer in $\text{SrCu}_2(\text{BO}_3)_2$ (left-hand panel) and the SS model (right-hand panel).

the excitation gap Δ is determined to be 35 K from the inelastic neutron scattering [12] and the electron spin resonance [13] experiments.

Secondly, excitations from the dimer singlet ground state in the SS model have extremely localized character. Using perturbation expansion in J'/J , Miyahara and Ueda [4] found that hopping of an excited triplet from one dimer to another is allowed only from sixth order. A very small dispersion width of 0.2 meV for the magnetic excitations was indeed observed by the neutron inelastic scattering experiments in $\text{SrCu}_2(\text{BO}_3)_2$ [12]. The most striking feature of $\text{SrCu}_2(\text{BO}_3)_2$ is the plateaus in the magnetization curve under high magnetic field at fractional values (1/8, 1/4 and 1/3) of the fully saturated magnetization [1, 14]. It is proposed that the small kinetic energy of the triplets and weak repulsive interaction between them are responsible for the formation of superstructure of triplet dimers at these plateaus [6, 7], although no direct experimental evidence has been obtained yet.

The nature of quantum phase transition in the SS model, however, is not well understood yet. Possibilities have been discussed for intermediate phases between the dimer singlet and the Néel state for a certain range of J'/J such as a plaquette-type singlet state [10] or a helical spin order [3]. The exchange parameters appropriate for $\text{SrCu}_2(\text{BO}_3)_2$ were estimated as $J = 85$ K and $J' = 54$ K ($J'/J = 0.64$) by fitting the magnetic susceptibility data to numerical simulation of the SS model [6]. Analysis of the energy of various excitation modes has lead to slightly different values, $J = 72$ K and $J' = 43$ K ($J'/J = 0.60$) [11]. For such parameter values, theories appear to agree that the ground state is the dimer singlet. Various properties of $\text{SrCu}_2(\text{BO}_3)_2$ known so far are indeed compatible with the dimer singlet ground state, although it may be in close proximity to a quantum critical transition.

In this letter, we report the results of nuclear magnetic resonance (NMR) experiments at ^{63}Cu and ^{11}B nuclei (both with nuclear spin 3/2) in $\text{SrCu}_2(\text{BO}_3)_2$. We observed fourfold splitting of Cu NMR lines and sinusoidal oscillation of Cu spin echo intensity against the separation time between the $\pi/2$ and π rf pulse. These phenomena are naturally explained by strong nuclear spin–spin coupling acting only within a pair, and therefore provide direct evidence for the dimer singlet ground state.

The NMR measurements were performed on a single crystal prepared by the travelling-solvent-floating-zone method and cut into an approximately cubic shape ($2.1 \times 2.3 \times 1.9$ mm³). The applied magnetic field H did not exceed 8 T; therefore, the Zeeman energy was much smaller than the excitation gap. The NMR spectra were obtained from the Fourier transform of the spin-echo signal. $\text{SrCu}_2(\text{BO}_3)_2$ has tetragonal structure with $I\bar{4}2m$ space group, in which $\text{Cu}(\text{BO}_3)$ and Sr layers stack alternately [15]. The atoms in the magnetic $\text{Cu}(\text{BO}_3)$ layer depicted in figure 1 are not strictly coplanar, and the only symmetry operation at either Cu

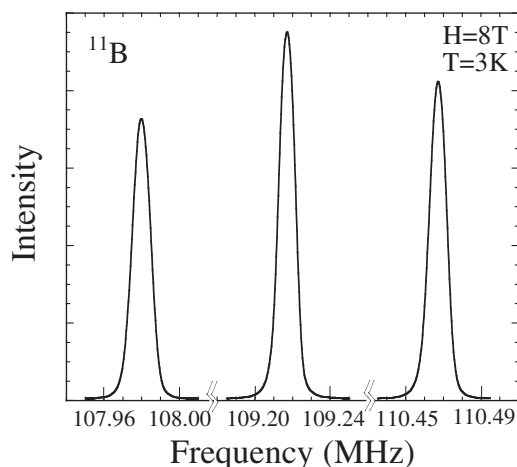


Figure 2. The ^{11}B spectrum at $T = 3$ K. The magnetic field is 7.9967 T parallel to the c -axis.

or B sites is the mirror reflection normal to $\langle 110 \rangle$. Then the direction normal to the mirror plane coincides with one of the principal axes of the electric field gradient (EFG) and the magnetic hyperfine shift (K -) tensors; however, neither possesses axial symmetry. When the magnetic field H is along the c -axis, the quadrupolar and the magnetic shifts are identical for all Cu (B) sites but the c -axis is not a principal axis of the EFG or K -tensors. For other field directions, there are more than two inequivalent sites. For example, there are two Cu (B) sites for $H \parallel [110]$. At one of these sites, H is normal to the mirror plane and thus along one of the principal axes of EFG and K -tensors.

Figure 2 shows the ^{11}B NMR spectrum at $T = 3$ K for $H = 7.9967$ T along the c -axis. The spectrum consists of three lines split by electric quadrupole interaction, yielding the quadrupole splitting $^{11}\nu_{cc} = ^{11}V_{cc}e^{11}Q/2h = 1.25$ MHz, where $^{11}V_{cc}$ is the cc -component of the EFG tensor and ^{11}Q is the nuclear quadrupole moment. Other components of quadrupole splitting are obtained from the spectrum for $H \parallel [110]$ as $^{11}\nu_{\alpha\alpha} = 0.694$ MHz and $^{11}\nu_{\beta\beta} = 0.555$ MHz, where α is a principal axis and β is perpendicular to it.

The ^{11}K magnetic hyperfine shifts at B sites along three directions c , α and β are determined from the position of the central line for the transition $I_z = 1/2 \leftrightarrow -1/2$ at $H = 8$ T. There are good linear relations between the shifts and the magnetic susceptibility χ , as shown in figure 3. From the slope of the K versus χ plot, three components of the hyperfine coupling tensor defined as $^{11}A_{ii} = ^{11}K_{ii}/(\mu_B N_A \chi_{ii})$ are determined as $^{11}A_{cc} = -0.259$, $^{11}A_{\alpha\alpha} = -0.202$ and $^{11}A_{\beta\beta} = 0.115$ in units of T/μ_B . The coupling constant $^{11}A_{ii}$ represents the i -component of the hyperfine field at B nuclei provided that each Cu has a uniform moment of $1 \mu_B$ along the i -direction. We found that the dipolar field from Cu spins alone does not account for the anisotropy of $^{11}A_{ii}$, indicating sizable anisotropy of the transferred hyperfine interaction. The temperature dependence of χ_{cc} is shown in the inset of figure 3. Since the susceptibility was measured at 1 T and the magnetization is not linear in field when the temperature is much lower than the gap, only the data above the peak temperature of χ are used in the K versus χ plot.

We now turn to the results at Cu sites. Figure 4 shows the ^{63}Cu NMR spectrum for the central transition at $H = 8.001$ T along the c -axis at $T = 3.0$ K. The spectrum consists of four equally spaced lines in spite of the fact that all Cu sites are equivalent for $H \parallel c$. Similar four-peak structure was observed for the quadrupole-split satellite spectra. The quadrupolar splitting for ^{63}Cu nuclei was obtained as $^{63}\nu_{cc} = 22.13$ MHz. As will be explained shortly,

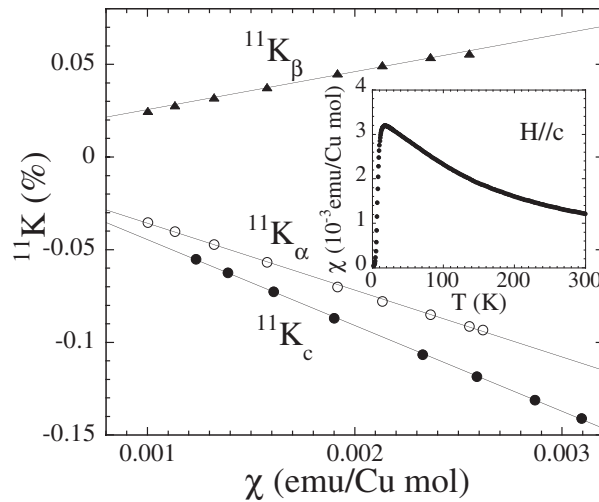


Figure 3. The shifts at B sites are plotted against the susceptibility. The solid lines show fitting to a linear relation.

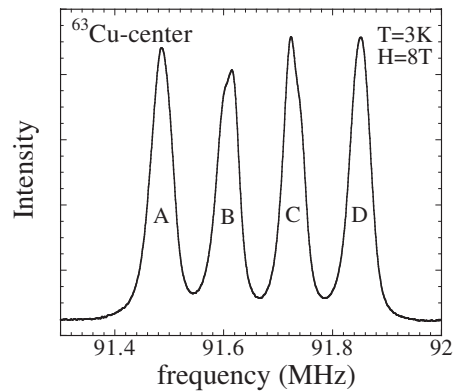


Figure 4. The ^{63}Cu NMR spectrum for the central line at $T = 3$ K. The magnetic field is 8.001 T parallel to the c -axis.

the fourfold splitting is due to the coupling of two Cu nuclear spins on the same dimer. The magnetic shift is then determined from the average frequency of the four peaks. The observation of Cu NMR signal is limited to $T \leq 4.2$ K because of the short spin–spin relaxation time at higher temperatures. The hyperfine coupling constant at Cu nuclei $^{63}A_{cc}$ was determined by plotting the shift for ^{63}Cu against the shift for ^{11}B , both taken at the same field and several temperatures below 4.2 K as shown in figure 5. From the slope of this plot and the value of $^{11}A_{cc}$ determined above, we obtain $^{63}A_{cc} = -23.76 \pm 0.15 \text{ T}/\mu_B$. Complete determination of the EFG and K -tensors at B and Cu sites will be presented in a separate paper.

We found remarkable oscillation of the spin-echo intensity of the ^{63}Cu resonance as shown in figure 6. Here the spin-echo intensity of peak B of the central line is plotted against twice the separation time τ between $\pi/2$ and π rf pulses. Such oscillation is observed only for peaks B and C. Similar oscillation was observed for the satellite spectra, although at different peaks. For the high-frequency satellite only peaks C and D show the echo oscillation, while for the low-frequency satellite oscillation was observed for peaks A and B.

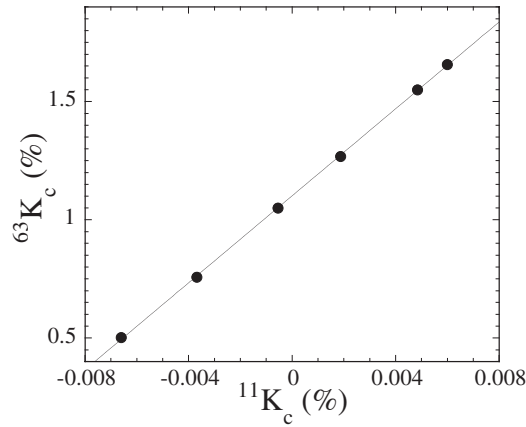


Figure 5. The magnetic hyperfine shift at Cu sites ($^{63}K_c$) is plotted against the shift at B sites ($^{11}K_c$). Both were taken at the same field, $H = 8$ T, along the c -axis in the temperature range below 4.2 K.

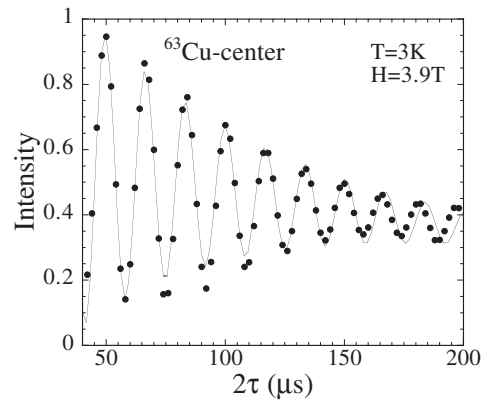


Figure 6. The spin-echo intensity of peak B in figure 4 for the centre line of the ^{63}Cu NMR spectrum is plotted as a function of 2τ , where τ is the separation time between $\pi/2$ and π pulses. The data are taken at $H = 3.9$ T along the c -axis and $T = 3$ K.

The line splitting and the echo oscillation are both explained easily by Rudermann–Kittel–Kasuya–Yosida-type indirect interaction between Cu nuclear spins mediated by the electron spin system. The indirect coupling between two nuclear spins I_1 and I_2 is generally expressed as [16]

$$H_{ind} = -a_z I_1^z I_2^z, \quad (1)$$

$$a_z = \hbar^2 \gamma_{N1} \gamma_{N2} (g_z A_z)^2 \chi_{12} \quad (2)$$

where γ_{N_i} is the nuclear gyromagnetic ratio for I_i and only the on-site hyperfine coupling constant along the field direction A_z is considered. The non-local electron spin susceptibility χ_{12} describes the spin polarization at site 1 when a fictitious magnetic field is applied only to the spin at site 2. At $T = 0$ this is expressed as

$$\chi_{12} = \sum_n \frac{\langle 0 | S_{2z} | n \rangle \langle n | S_{1z} | 0 \rangle}{E_n} + \text{c.c.}, \quad (3)$$

where $|0\rangle$ is the ground state and $|n\rangle$ is an excited state with energy E_n . In the case of an isolated dimer with exchange J ,

$$\chi_{12} = -\frac{1}{2J}. \quad (4)$$

Equation (1) implies that local magnetic field acting on I_1 is produced by I_{2z} , which can take four different values $\pm 1/2$ or $\pm 3/2$. This results in the fourfold splitting of the NMR line for I_1 . Since I_2 can be either of the two isotopes ^{63}Cu or ^{65}Cu , there should strictly speaking be eightfold splitting. However, both isotopes have spin $3/2$ and the difference in γ is only 7%. Thus they are not experimentally resolved. Assuming that the spectrum in figure 4 represents the isotopic average for I_2 , the value of a_z for the case when I_2 is a ^{63}Cu nucleus is deduced as $a_z/h = 119$ kHz.

It is well known that such a nuclear spin coupling gives rise to spin-echo oscillation [17]

$$I(2\tau) = \cos(a_z\tau/\hbar) \quad (5)$$

when the two spins are identical (like spins). Because of the quadrupole splitting, only those ^{63}Cu nuclei with $I_z = \pm 1/2$ behave as like spins when the central line for the transition $I_z = 1/2 \leftrightarrow -1/2$ is being observed. This is why only peaks B and C show oscillation. The selection rules for the satellite lines is explained in a similar manner. The data in figure 6 are fitted to a sum of oscillatory and non-oscillatory parts, both decaying exponentially with different time constants. The oscillation frequency is obtained as $a_z/h = 119$ kHz, in agreement with the value deduced from the splitting of the spectrum.

The fourfold splitting of the spectrum and the coherent spin-echo oscillation indicate that nuclear spins are strongly coupled in pairs and the couplings between pairs are very weak. The results thus provide direct evidence for the dimer singlet ground state in $\text{SrCu}_2(\text{BO}_3)_2$. If one nucleus were coupled to many neighbours, for example as one would expect for the plaquette-type singlet state, the spectrum should consist of many lines, which with random isotopic configuration would result in a single broad peak. Likewise, random superposition of echo oscillation containing many frequency components would show rapid damping. The long-lived coherent echo oscillation implies that the inter-dimer coupling if any is orders of magnitude smaller than the intra-dimer coupling. Similar phenomena have been observed also for the chain Cu sites in the ladder-chain composite material $\text{Sr}_{14}\text{Cu}_{24}\text{O}_{41}$, where the dimer singlet state is formed due to charge order in the one-dimensional chain subsystem [18].

For the case of an isolated dimer, the coupling constant $a_z/h = 119$ kHz corresponds to the exchange constant $J = 75$ K. Here we have used equations (1), (2) and (4) with the values $A_c = -23.76 \text{ T}/\mu_B$ and $g_c = 2.28$, the latter being obtained from the ESR measurements [13]. This value of J is remarkably close to the intra-dimer exchange estimated for $\text{SrCu}_2(\text{BO}_3)_2$. Although J'/J is not a small number for $\text{SrCu}_2(\text{BO}_3)_2$, the spin correlation within a dimer must remain almost unchanged from an isolated dimer.

In conclusion, ^{63}Cu and B NMR measurement has been performed on a single crystal of $\text{SrCu}_2(\text{BO}_3)_2$. The values of the hyperfine coupling constant and the quadrupole splitting were determined. The spectrum of Cu splits into four lines and the spin-echo intensity oscillates against 2τ with the oscillation frequency equal to the line splitting. These are caused by the nuclear spin-spin coupling mediated by the strong intradimer coupling of the electron spins. These results provide firm evidence that the ground state is indeed the dimer singlet state.

This work was supported by Grant-in Aid for Scientific Research 10304027 from the Japanese Society of the Promotion of Science and Priority Area (A) on 'Novel quantum phenomena in transition metal oxides' and Priority Area (B) on 'Field-induced new quantum phenomena in magnetic systems' from the Ministry of Education, Culture, Sports, Science and Technology of Japan.

References

- [1] Kageyama H, Yoshimura K, Stern R, Mushnikov N V, Kato M, Kosuge K, Slichter C P, Goto T and Ueda Y 1999 *Phys. Rev. Lett.* **82** 3168
- [2] Shastry B S and Sutherland B 1981 *Physica B* **108** 1069
- [3] Mila F and Albrecht M 1996 *Europhys. Lett.* **34** 145
- [4] Miyahara S and Ueda K 1999 *Phys. Rev. Lett.* **82** 3701
- [5] Weihong Z, Hamer C J and Oitma J 1999 *Phys. Rev. B* **60** 6608
- [6] Miyahara S and Ueda K 2000 *Phys. Rev. B* **61** 3417
- [7] Momoi T and Totsuka K 2000 *Phys. Rev. B* **61** 3231
Momoi T and Totsuka K 2000 *Phys. Rev. B* **62** 15 067
- [8] Miyahara S and Ueda K 2000 *J. Phys. Soc. Japan Suppl. B* **69** 72
- [9] Müller-Hartmann E, Singh R R P, Knetter C and Uhrig G S 2000 *Phys. Rev. Lett.* **84** 1808
- [10] Koga A and Kawakami N 2000 *Phys. Rev. Lett.* **84** 4461
- [11] Knetter C, Bühler A, Müller-Hartmann E and Uhrig G S 2000 *Phys. Rev. Lett.* **85** 3958
- [12] Kageyama H, Nishi M, Aso N, Onizuka K, Yoshihama T, Nukui K, Kodama K, Kakurai K and Ueda Y 2000 *Phys. Rev. Lett.* **84** 5876
- [13] Nojiri H, Kageyama H, Onizuka K, Ueda Y and Motokawa M 1999 *J. Phys. Soc. Japan* **68** 2906
- [14] Onizuka K, Kageyama H, Ueda Y, Goto T, Narumi Y and Kindo K 2000 *J. Phys. Soc. Japan* **69** 1016
- [15] Smith R W and Keszler D A 1991 *J. Solid State Chem.* **93** 430
- [16] Takigawa M 1994 *Phys. Rev. B* **49** 4158
- [17] Abragham A 1961 *The Principles of Nuclear Magnetism* (Oxford: Oxford University Press) p 497
- [18] Takigawa M, Motoyama N, Eisaki H and Uchida S 1998 *Phys. Rev. B* **57** 1124